frontiers | Frontiers in Astronomy and Space Sciences

TYPE Original Research
PUBLISHED 15 July 2024
DOI 10.3389/fspas.2024.1402031

OPEN ACCESS

EDITED BY
Jadwiga Daszynska-Daszkiewicz,
University of Wrocław, Poland

REVIEWED BY
Andrzej S Baran,
Missouri State University, United States
Mkrtichian Egishe David,
National Astronomical Research Institute of Thailand, Thailand

*CORRESPONDENCE
Lin-Qiao Jiang,
jianglinqiao11@163.com

RECEIVED 16 March 2024
ACCEPTED 30 May 2024
PUBLISHED 15 July 2024

CITATION
Jiang L-Q and Zheng J (2024), Investigation of a W UMa-type contact binary GZ And in a physical triple system.
Front. Astron. Space Sci. 11:1402031.
doi: 10.3389/fspas.2024.1402031

Investigation of a W UMa-type contact binary GZ And in a physical triple system

Lin-Qiao Jiang [1,2,3]* and Jie Zheng [4]

[1]School of Science, Leshan Normal University, Leshan, China, [2]Center for Applied Optics Research, Leshan Normal University, Leshan, China, [3]Key Laboratory of Detection and Application of Space Effect in Southwest Sichuan, Leshan, China, [4]CAS Key Laboratory of Optical Astronomy, National Astronomical Observatories, Chinese Academy of Sciences, Beijing, China

GZ And is a variable star within the visually observed multiple-star system ADS 1693. Recent observations have yielded new light curves for GZ And, obtained using the Xinglong 85-cm telescope and the Transiting Exoplanet Survey Satellite (TESS) satellite. These light curves, along with radial velocity curves, were analyzed simultaneously to ascertain the fundamental physical parameters of GZ And's components. The findings indicate that the primary star has a mass of $M_1 = 0.57(4)M_\odot$, radius of $R_1 = 0.75(2)R_\odot$, and luminosity of $L_1 = 0.42(2)L_\odot$. The secondary star is characterized by a mass of $M_2 = 1.19(9)M_\odot$, radius of $R_2 = 1.04(3)R_\odot$, and luminosity of $L_2 = 0.63(3)L_\odot$. Their orbital separation is determined to be $a = 2.30(6)R_\odot$. An analysis of the accumulated times of light minima reveals that GZ And is undergoing orbital period variations at a rate of $dP/dt = -7.58(7) \times 10^{-8} day \cdot year^{-1}$, likely due to mass transfer from the more massive component to its lighter counterpart at a rate of $dM_2/dt = -9.06(8) \times 10^{-8} M_\odot \cdot year^{-1}$. Additionally, distance measurements for the component stars in ADS 1693, derived from Gaia DR3 astrometric data, suggest that ADS 1693A (GZ And) and ADS 1693B are gravitationally bound and likely originated from the same molecular cloud, sharing similar ages. This evidence supports the classification of GZ And as a W UMa-type contact binary within a physically associated triple system.

KEYWORDS

multiple stars, eclipsing binary stars, contact binary stars, fundamental parameters of stars, solar-like stars: fundamental parameters

1 Introduction

More than half of the stars in the universe are part of binary or multiple stellar systems. However, only a fraction of these systems exhibit eclipses observable from the Earth (Guinan, 2004). Eclipsing binaries serve as fundamental building blocks in stellar astrophysics, allowing the determination of the masses and radii of the component stars through photometric and spectroscopic observations (Torres et al., 2010). Over recent decades, tens of thousands of eclipsing binaries have been identified using these methods. Notably, Slawson et al. (2011) unveiled the Second Data Release of Kepler Eclipsing Binary Stars, encapsulating 2,165 eclipsing binaries with remarkably precise light curves. Additionally, Prša et al. (2022) cataloged 4,584 eclipsing binaries identified in the initial 2-year sky survey conducted by the Transiting Exoplanet Survey Satellite (TESS) (Ricker et al., 2015). Complementarily, Qian et al. (2017), Qian et al. (2018) compiled data on 7,938 EW-type and 3,196 EA-type eclipsing binaries, as observed by the Large Sky Area Multi-Object Fiber Spectroscopic

Telescope (LAMOST, also known as the Guo Shoujing Telescope), employing a low-resolution spectrograph (LRS) (Cui et al., 2012; Zhao et al., 2012). In a more recent advancement, Mowlavi et al. (2023) introduced the first Gaia catalog of eclipsing binary candidates in Gaia Data Release 3 (Gaia DR3), encompassing over 2,184,477 candidates across a brightnesses range in the Gaia G-band from a few to 20 magnitudes covering the entire sky. These efforts signify a promising advancement in the research of eclipsing binaries, demonstrating a growing interest and expanding knowledge base in this field.

Recent intensive studies have shown that many eclipsing binaries are part of more complex systems, often including three or more stars (Duchêne and Kraus, 2013). In an in-depth survey of 165 solar-type spectroscopic binaries, Tokovinin et al. (2006) examined the impact of higher-order multiplicity on orbital period distributions. Their findings highlighted notable differences between the orbital period distributions of spectroscopic binaries with and without tertiary companions, suggesting that tertiary companions might influence the primary binary's orbital period through angular momentum exchange via the Kozai mechanism (Kozai, 1962). Furthermore, Zhou et al. (2019) suggested that dynamic interactions within these systems, particularly between the eclipsing binary and any additional companions, could alter the binary's orbital period. Delving into specific cases offers further insights into these complex relationships. Welsh et al. (2012) disclosed that the systems Kepler-34 and Kepler-35 both harbor circumbinary planets, providing compelling examples of the diverse architectures within stellar systems. Meanwhile, Wang and Zhu (2021) raised the intriguing possibility of an undetected black hole in orbit around the eclipsing binary RR Dra, underscoring the vast range of celestial phenomena yet to be fully understood. These investigations shed light on the intricate dynamics of multiple-star systems.

The study of GZ And, a member of the visual multiple system ADS 1693, spans nearly a century. Initially, as shown in Figure 1, ADS 1693 was determined to comprise four components: ADS 1693A, B, C, and D, with GZ And (ADS 1693A) being identified as the brightest. Espin (1908) made early visual observations of the system's variability but could not definitively attribute the brightness changes to either ADS 1693A or B. Subsequently, Walker (1973) analyzed the *UBV* band light curves of ADS 1693A, identifying it as a W UMa-type binary with a spectral type of G7 or K0, and confirmed that the other components—ADS 1693B, C, and D—were not variable, classifying their spectral types as G5, K4, and G7 based on their color indices. This led to the conclusion that ADS 1693 is a quintuplet system. GZ And was then designated as ADS 1693A (Kukarkin et al., 1975). Further light curve analyses by Liu et al. (1987) reconfirmed its EW-type binary classification. Walker's (1991, 1996) measurements indicated that ADS 1693B, C, and D were positioned 8, 13, and 24 arcseconds away from A, respectively, suggesting that GZ And is part of a close triple system, with the wider pair orbiting approximately every 5.3 years. Although Liu et al. (1987) made these claims, comprehensive photometric solutions and power spectrum analyses are not available now. Later, Lu and Rucinski (1999) unveiled radial velocity curves of GZ And, indicating it as a W-subtype contact binary with a mass ratio of q = 0.514 (08), but did not detect a third component spectroscopically. While both Yang and Liu (2003) and Baran et al. (2004) provided photometric solutions for GZ And, this intriguing visual multiple system still demands further in-depth research to unravel its complexities fully.

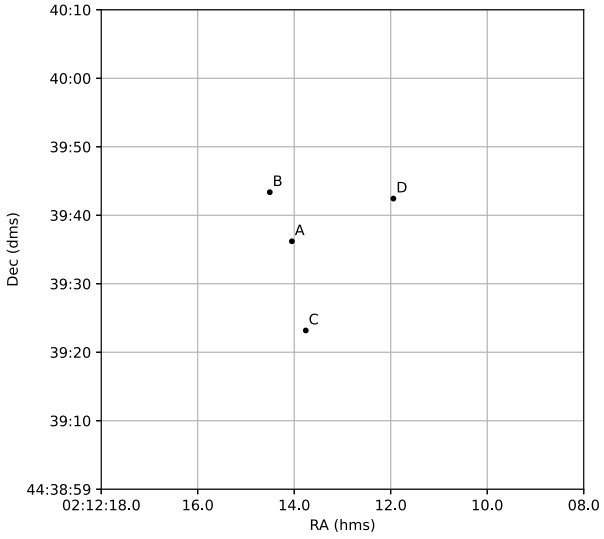

FIGURE 1
Star map of GZ And.

This study unveils new findings on the W UMa-type contact binary GZ And, situated within a visual multiple system. Section 2 details the photometric data employed in our subsequent analyses. In Section 3, we analyze the $O-C$ curve of the light minima timings to ascertain the orbital period changes of GZ And. Section 4 is dedicated to deriving the photometric solutions for the binary system by fitting its observed light curves. Finally, in Section 5, we discuss our findings and present the conclusions drawn from our analyses.

2 Observations

2.1 Ground-based observations

The BVR_cI_c light curves of GZ And were observed using the Xinglong 85-cm telescope on 16 November 2022 (Zhou et al., 2009). This telescope is situated at the Xinglong Observatory, which is part of the National Astronomical Observatories, Chinese Academy of Sciences (NAOC), designated by the IAU code 327 and located at 40°23′39″.0 N, 117°34′30″.0 E. An Andor DZ936N 4K CCD camera was attached to the telescope, along with a standard Johnson-Cousins-Bessel multicolor filter system. The observational session involved an exposure time of 20 s for the B filter, 12 s for the V filter, and 10 s for each of the R_c and I_c filters, resulting in 360 images per filter. Subsequent observations of GZ And were conducted again using the Xinglong 85-cm telescope on 13 November 2023, utilizing only the V filter with a 15-s exposure time, yielding a total of 1,262 images. The images were processed using our own Quick Light-Curve Pipeline (QLCP) in standard mode.[1] QLCP is an automated light-curve extractor for raw photometric images.

1 https://gitee.com/drjiezheng/qlcp

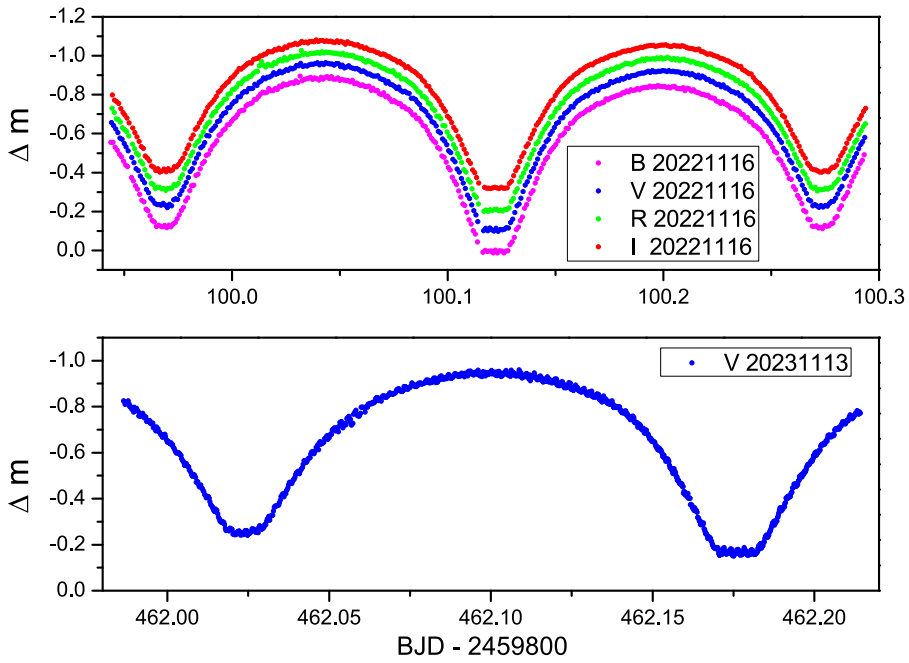

FIGURE 2
Photometric observations taken with the Xinglong 85-cm telescope.

It performs bias and flat corrections, as well as image alignment. The mature program, Source-Extractor (Bertin and Arnouts, 1996), was then used to extract sources and measure their flux. Finally, the differential calibrated light curves are generated. All the light curves are depicted in Figure 2. From the initial session in 2022, we derived one primary and two secondary times of light minima. From the subsequent session in 2023, one primary time and one secondary time of light minima were identified. These times are tabulated in Supplementary Table S1.

2.2 TESS observations

The Transiting Exoplanet Survey Satellite (TESS), a NASA mission led by MIT, aims to detect transiting events through an all-sky survey (Ricker et al., 2015). GZ And was initially monitored during the TESS Prime Mission in Sector 18 with an 1800-s observation cadence as TIC 292612740. Subsequently, in the mission's fifth year, GZ And was observed again in Sector 58. The data in Sector 58 were retrieved using the Python package `lightkurve` (Collaboration et al., 2018) from the MAST data archive,[2] which provides two different types of data products. One is the light curve from the author named QLP with an exposure time of 200 s, and the other is the cutouts of the calibrated full-frame images from the author named TESScut with an exposure time of 158.4 s. We downloaded 20 × 20 pixel files centered on GZ And using the `TESScut` tool. Then, the Python procedure `dat.to_lightcurve` was used to get simple aperture photometry light curve, and the flux data were normalized and transformed into magnitudes. The results are presented in Figure 3. It should be noted that these data were not compared to a constant star to make them differential. From the TESS light curve, a total of 175 times of light minima were identified, as detailed in Supplementary Table S1. Notably, the TESS observations managed to completely cover the orbital phase corresponding to the observations made with the Xinglong 85-cm telescope on 16 November 2022.

3 Variations of the orbital period

Orbital period variations are a common phenomenon in close binary systems, typically resulting from mass transfer between components, the gravitational influence of distant stellar or substellar companions, and other factors (Zhou et al., 2016; Zhou and Soonthornthum, 2019). The O-C method is commonly used to analyze orbital period variations, in which O refers to observed times of light minima and C refers to calculated times of light minima while a designated reference epoch is given. The observed data covering light minima, as shown in Figures 2 and 3, are fitted by a parabola with the least squares method to determine the observed times of light minima. Then, we compiled all previously published times of light minima and included them in the Supplementary Material, alongside the minima determined from our observations and TESS data, to analyze the orbital period changes of GZ And.

A linear ephemeris,

$$Min.I(BJD) = 2459900.121896\,(30) + 0^{d}.3050173 \times E, \quad (1)$$

2 https://archive.stsci.edu/

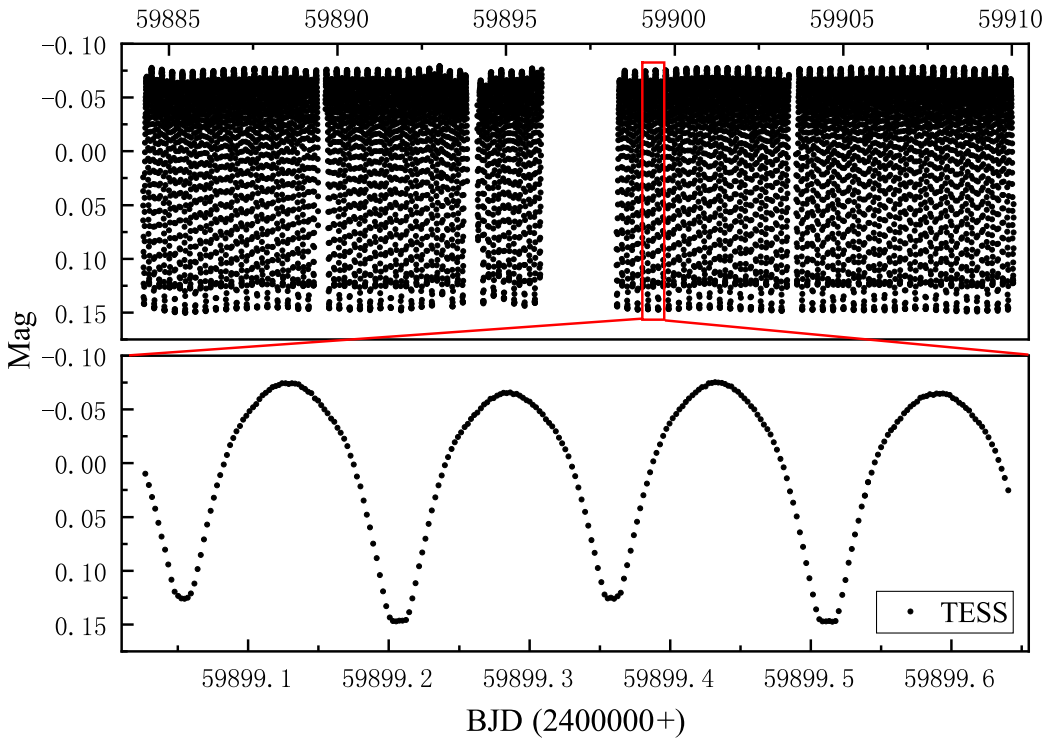

FIGURE 3
Light curves collected with TESS in Sector 58.

serves as the basis for calculating the O–C (observed minus calculated) values. We used Eq. 1, where the time of the primary light minimum observed by the Xinglong 85-cm telescope is designated as the reference epoch. An initial orbital period of p = 0.3050173 days, sourced from the *O-C gateway*,[3] was utilized. The computed O–C values are graphically depicted in Figure 4: black dots illustrate data from the existing literature, while red and green dots correspond to findings from TESS and the Xinglong 85-cm telescope, respectively. Observing a downward parabolic trend in the O-C data, we applied a quadratic polynomial to fit the O-C curve. Due to some uncertainties not accounted for in Supplementary Table S1, we assigned equal weight to each data point during the fitting process. The resulting equation (Eqs 2, 3) is

$$O-C = -1.8\,(\pm 0.8)\times 10^{-4} - 1.78\,(\pm 0.01)\times 10^{-6}\times E - 3.16\\ (\pm 0.03)\times 10^{-11}\times E^{2}. \quad (2)$$

Subsequently, the ephemeris was refined to

$$Min.I\,(BJD) = 2459900.1217 + 0^{d}.3050155\times E. \quad (3)$$

The orbital period of GZ And shortens at a rate of $dP/dt = -7.58(7)\times 10^{-8} day\cdot year^{-1}$, indicating a continuous decrease in the system's orbital period. The parabolic fit, depicted with black solid lines, is also presented in Figure 4 for comparison. Since only a few times of light minima are obtained before BJD 2446016, and the same weight was given to all O-C values while fitting the O-C curve, the O-C values prior to −40000 are not fitted well, as shown in Figure 4.

4 Synthesis of the light curve

The Wilson–Devinney (W-D) code (Wilson and Devinney, 1971; Wilson and Van Hamme, 2014) was employed to model the light curves collected using the Xinglong 85-cm telescope and TESS. The light curve morphology of GZ And is classified as EW type, which corresponds to contact binaries. Consequently, we applied mode 3, designated for overcontact binaries, in our analysis. For the star undergoing primary eclipses (commonly referred to as the primary star or star 1), we set its surface effective temperature at T_1 = 5348 K, a value sourced from Gaia DR3 (Gaia et al., 2016; Gaia et al., 2023). Although this temperature cannot be verified at which phase of the GZ And orbit, previous studies from other researchers (Walker, 1973) and Gaia data indicate that GZ And is a solar-type contact binary. Even though the actual temperature of the primary star may be several hundred degrees higher or lower, changes to the determined parameters such as orbital inclination, mass ratio, and the temperature ratio between two components will be minimal, as they mainly rely on the variations of the light curve (Jiang et al., 2015). Given that GZ And is akin to a solar-type system, we presume the presence of convective envelopes for both stars. Accordingly, we assigned bolometric albedos of A_1 = 0.5 and A_2 = 0.5 (Ruciński, 1969) for the respective components. The gravity-darkening coefficients are established at g_1 = 0.32

3 http://var2.astro.cz/ocgate/

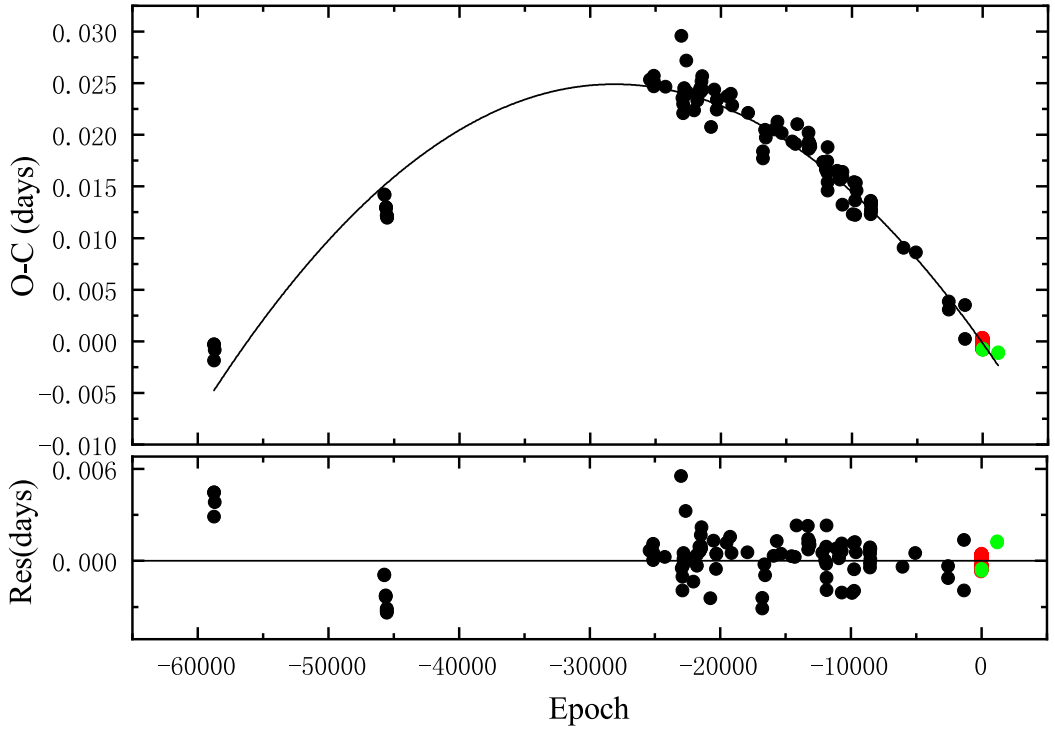

FIGURE 4
O-C diagram.

and g_2 = 0.32 (Lucy, 1967), reflecting the behavior of convective stellar envelopes. For limb-darkening coefficients, we selected the monochromatic, passband-specific, and bolometric coefficients as per the values listed in van Hamme's (1993) tables.

With the radial velocity curves for GZ And already provided by Lu and Rucinski (1999), there was no necessity to use the q-search method to determine the mass ratio (q) of the binary system. In our analysis using the W-D program, we concurrently fit Lu and Rucinski's (1999) radial velocity curve along with the BVR_cI_c light curves from the Xinglong 85-cm optical telescope and the TESS light curve. We synchronized our study with the TESS light curve observed on 16 November 2022, matching the observation date of the Xinglong telescope's BVR_cI_c light curves. The primary adjustable parameters in our model include orbital semi-major axis in solar radii (A), systemic radial velocity (V_γ), star 2 average surface temperature (T_2), the mass ratio (q) of the binary system, orbital inclination (i) observed from Earth, the modified dimensionless surface potential of star 1 (Ω_1), and passband-specific luminosities (L_1). Notably, as illustrated in Figures 6 and 7, the observed light curves exhibit asymmetry, a characteristic often associated with the O'Connell effect (O'Connell, 1951), prevalent in contact binaries of solar or later spectral types, typically attributed to stellar magnetic activity (Kouzuma, 2019). To accommodate this asymmetry, spot parameters are integrated as variable components in our model, encompassing the spot's latitude, longitude, angular radius, and temperature factor. Given the correlation between angular radius and temperature factor, only one is varied during the fitting process. We also explored the inclusion of the third light (l_3) as an adjustable parameter, yet the findings confirmed the absence of tertiary luminosity contribution in GZ And. The solutions are tabulated in Table 1, with the observed and synthesized radial velocity and light curves showcased in Figures 5–7. The mass ratio listed in Table 1 is nearly the reciprocal of the value given by Lu and Rucinski (1999) since we used the opposite designation of primary and secondary stars. The geometric structure of the primary and secondary stars at phase 0 and phase 0.5, depicted in Figure 8, clearly demonstrates GZ And's total eclipse nature, with the secondary star's spot illustrated in dark black.

5 Discussion and conclusion

The photometric analyses presented in Table 1 characterize GZ And as a W-subtype shallow contact binary system with a filling factor of f = 14(2)%. The system demonstrates a notably high orbital inclination of i = 89.99°, enabling the primary star's total eclipse at orbital phase 0, vividly depicted in Figure 8. The credibility of the solutions in Table 1 is reinforced by their derivation from comprehensive radial velocity curves and fully eclipsed light curves, ensuring their dependability. Using the mass function $(M_1 + M_2)sin^3 i = 1.763(44)M_\odot$ (Lu and Rucinski, 1999), along with the given orbital inclination of i = 89.99° and mass ratio $M_2/M_1 = 2.07(1)$, we determined the masses of the component stars: $M_1 = 0.57(4)M_\odot$ for the primary and $M_2 = 1.19(9)M_\odot$ for the secondary. By applying Kepler's third law, we can articulate the following equation:

$$\frac{a^3}{P^2} = \frac{G}{4\pi^2} \times (M_1 + M_2). \quad (4)$$

TABLE 1 Photometric solutions of GZ And.

Parameter	Value
Mode	Overcontact binary
Orbital inclination i(°)	89.99 (6)
Mass ratio M_2/M_1	2.07 (1)
Primary temperature T_1 (K)	5348 (fixed)
Secondary temperature T_2 (K)	5038 (3)
Temperature ratio T_2/T_1	0.9420 (5)
Orbital semi-major axis in solar radii A	2.32 (12)
Systemic radial velocity v_γ	−4.01 (6)
Luminosity ratio $L_1/(L_1+L_2)$ in band B	0.4433 (7)
Luminosity ratio $L_2/(L_1+L_2)$ in band B	0.5567 (7)
Luminosity ratio $L_1/(L_1+L_2)$ in band V	0.4201 (6)
Luminosity ratio $L_2/(L_1+L_2)$ in band V	0.5799 (6)
Luminosity ratio $L_1/(L_1+L_2)$ in band R_c	0.4057 (6)
Luminosity ratio $L_2/(L_1+L_2)$ in band R_c	0.5943 (6)
Luminosity ratio $L_1/(L_1+L_2)$ in band I_c	0.3959 (6)
Luminosity ratio $L_2/(L_1+L_2)$ in band I_c	0.6041 (6)
Luminosity ratio $L_1/(L_1+L_2)$ in band TESS	0.3974 (10)
Luminosity ratio $L_2/(L_1+L_2)$ in band TESS	0.6026 (10)
Modified dimensionless surface potential of star 1	5.27 (1)
Modified dimensionless surface potential of star 2	5.27 (1)
Filling factor	0.14 (2)
Radius of star 1 (relative to the semi-major axis) in the pole direction	0.3045 (3)
Radius of star 2 (relative to the semi-major axis) in the pole direction	0.4241 (13)
Radius of star 1 (relative to the semi-major axis) in the side direction	0.3189 (4)
Radius of star 2 (relative to the semi-major axis) in the side direction	0.4523 (17)
Radius of star 1 (relative to the semi-major axis) in the back direction	0.3565 (4)
Radius of star 2 (relative to the semi-major axis) in the back direction	0.4829 (24)
Equal-volume radius of star 1 (relative to the semi-major axis) R_1	0.3285 (2)
Equal-volume radius of star 2 (relative to the semi-major axis) R_2	0.4551 (10)
Radius ratio R_2/R_1	1.385 (3)
Roche lobe equal-volume radius of star 1 (relative to the semi-major axis)	0.3180 (3)
Roche lobe equal-volume radius of star 2 (relative to the semi-major axis)	0.4431 (4)
Density of star 1 (in unit of sun 1410.0408422881391743 kg/m^3)	1.325 (4)
Density of star 2 (in unit of sun 1410.0408422881391743 kg/m^3)	1.03 (1)
Spot latitude in radians	2.28 (9)
Spot longitude in radians	1.55 (2)
Spot angular radius in radians	0.39422 (fixed)
Spot dimensionless temperature factor	0.88 (2)

(Continued on the following page)

Consequently, the orbital semi-major axis of GZ And is determined to be $a = 2.30(6)R_\odot$. The calculated radii and luminosities of the two-component stars are as follows: $R_1 = 0.75(2)R_\odot$, $R_2 = 1.04(3)R_\odot$, $L_1 = 0.42(2)L_\odot$, and $L_2 = 0.63(3)L_\odot$. Typically, in contact binary systems, the components, enveloped within a common atmosphere, exhibit nearly identical temperatures. Yet, the noted temperature disparity of $310K$ between the two stars, coupled with the modest filling factor of 14%, suggests that GZ And could represent an incipient contact binary system that has not yet attained thermal equilibrium (Zhou et al., 2015; Wang et al., 2022).

The analysis of the orbital period reveals a decreasing trend for GZ And, quantified at $dP/dt = -7.58(7) \times 10^{-8} day \cdot year^{-1}$. This decline is likely due to mass transfer from the more massive secondary star to the less massive primary star. Under the assumption of conservative mass transfer, the transfer rate can be calculated using the following equation:

$$\frac{dM_2}{dt} = -\frac{M_1 M_2}{3P(M_1 - M_2)} \times dP/dt. \quad (5)$$

Based on this, the mass transfer rate is determined to be $\frac{dM_2}{dt} = -9.06(8) \times 10^{-8} M_\odot/year$. However, it is important to note that the actual mass transfer rate might significantly differ when the effects of angular momentum loss are taken into account. Furthermore, the observed parabolic variations in the orbital period, depicted in Figure 4, could potentially be attributed to the light-travel time effect, which arises due to the presence of close stellar companions within the ADS 1693 visual multiple system in which GZ And resides.

While multiple stellar systems are prevalent across our skies, the subset featuring eclipsing binaries within such systems is relatively rare (Chambliss, 1992). These configurations offer unique insights into the dynamic interactions and evolutionary processeswithin

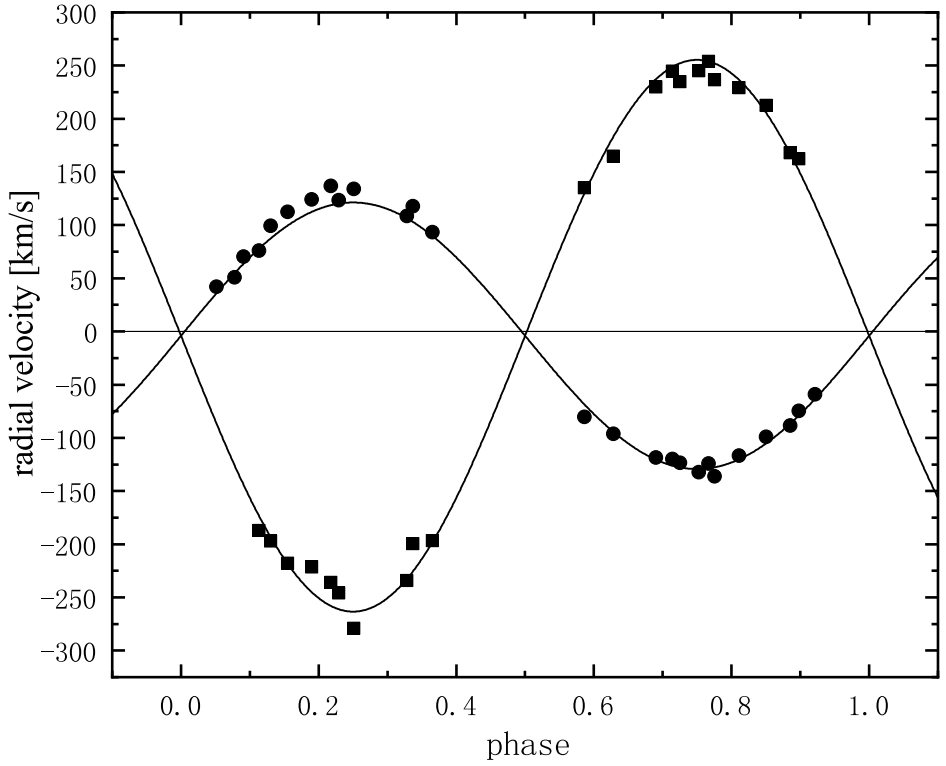

FIGURE 5
Radial velocity curves.

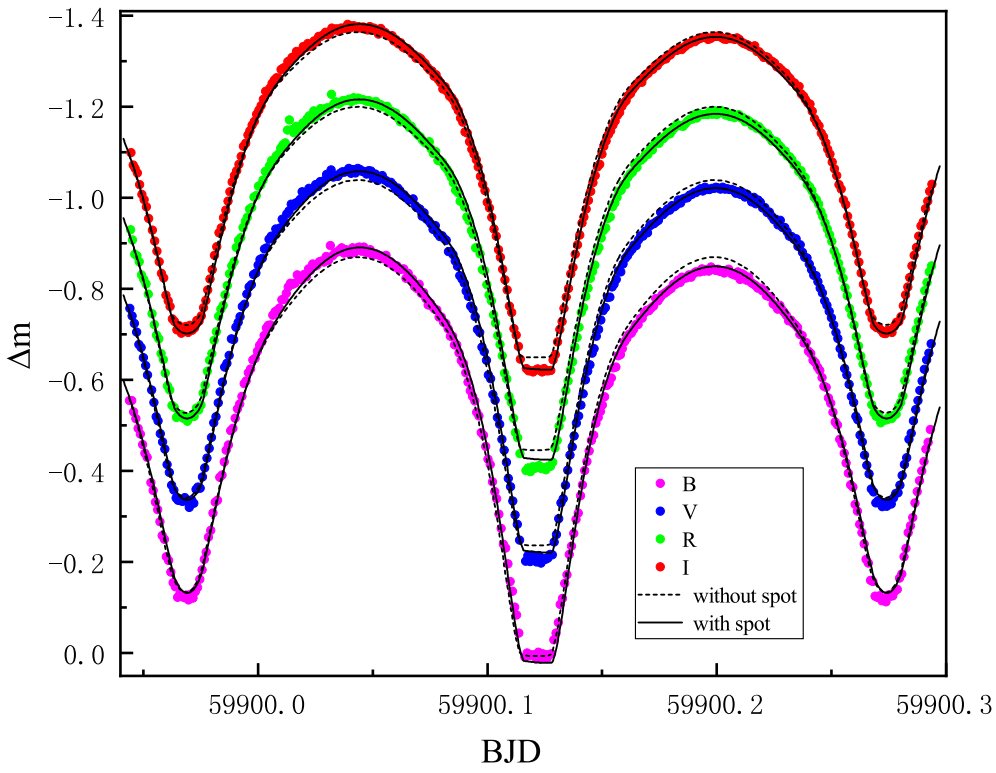

FIGURE 6
BVR_cI_c light curves.

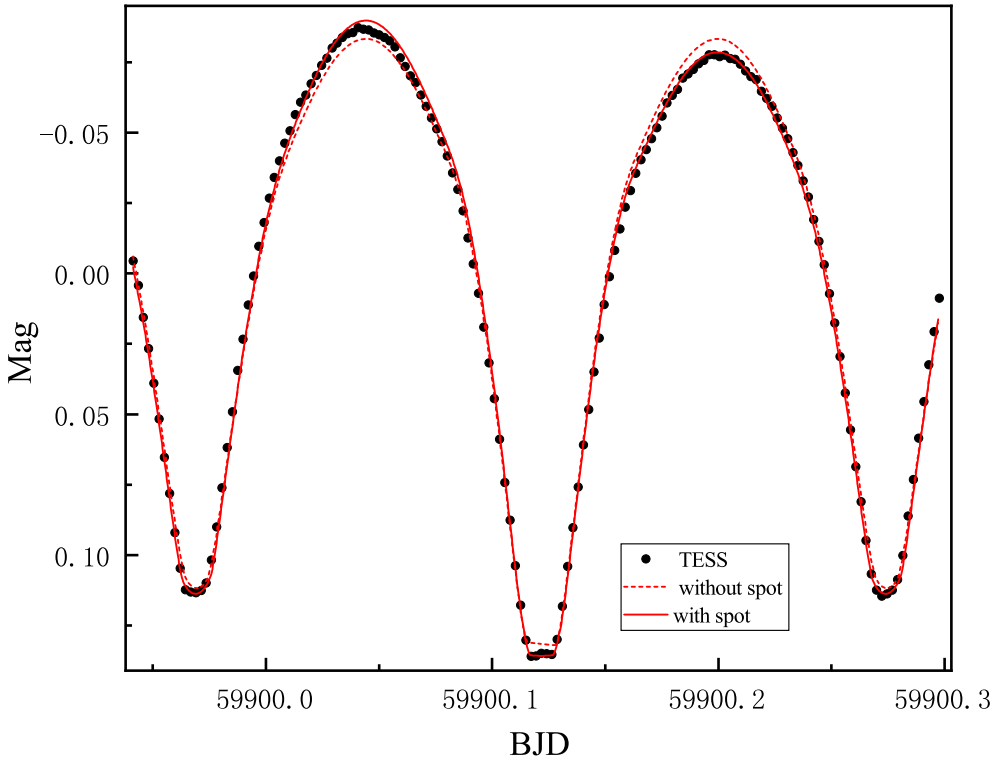

FIGURE 7
TESS light curves.

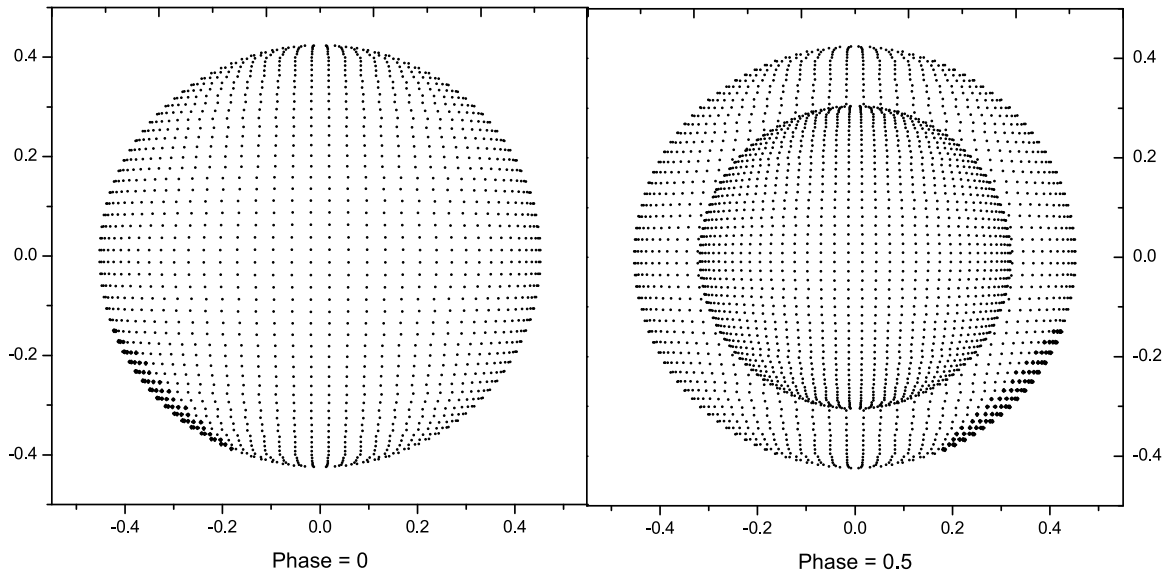

FIGURE 8
Geometric structure of GZ And.

multiple stellar systems. Walker (1991, 1996) posited that GZ And resides within the quintuple system ADS 1693, although detailed results of this claim are pending. Gaia mission observations have provided astrometric data for this system, as documented in Gaia DR3 and summarized in Table 2. Analysis indicates that ADS 1693A (GZ And) and ADS 1693B share close proximities in distance to Earth, suggesting a potential gravitational binding between the two.

TABLE 2 Data from Gaia DR3.

Name	Name	Parallax	Teff	*logg*	[Fe/H]	Distance
		mas	*K*	cm/s^2	*dex*	*pc*
ADS 1693A	GZ And	5.94 (2)	5348^{-78}_{+64}	$4.30^{-0.02}_{+0.01}$	$-0.269^{-0.076}_{+0.083}$	$167.6^{-0.5}_{+0.5}$
ADS 1693B	UCAC2 47016021	6.03 (8)	5802^{-32}_{+15}	$4.29^{-0.04}_{+0.06}$	$-0.285^{-0.020}_{+0.010}$	$184.0^{-13.6}_{+9.8}$
ADS 1693C	2MASS J02121375 + 4439231	0.62 (2)	4931^{-3}_{+5}	$2.58^{-0.01}_{+0}$	$-0.101^{-0.002}_{+0.002}$	$1989.8^{-10.1}_{+16.7}$
ADS 1693D	2MASS J02121194 + 4439424	1.73 (3)	5879^{-16}_{+14}	$4.06^{-0.17}_{+0.04}$	$-0.291^{-0.015}_{+0.013}$	$611.1^{-42.9}_{+172}$

Considering that the parabolic fit in Figure 4 could be a part of a periodic variation caused by a tertiary, the distance between ADS 1693A and ADS 1693B is estimated to be approximately $1340.7 AU$, based on their separation of 8 arcseconds (Walker, 1991; 1996), and a distance of 167.6 *pc* from Earth. Using Kepler's third law and assuming the mass of ADS 1693B is $1\,M_{\odot}$, the orbital period of ADS 1693B around ADS 1693A is estimated to be $2.95 \times 10^4 years$. The period is significantly longer than the time span covered in Figure 4, reinforcing the possibility that ADS 1693A (GZ And) and ADS 1693B are gravitationally bound.

Conversely, ADS 1693C and ADS 1693D appear significantly more distant from GZ And, likely positioning them as background stars along the same line of sight rather than integral system components. An intriguing aspect is the similarity in surface gravity and metallicity between ADS 1693A and ADS 1693B, hinting at a common origin from the same molecular cloud and nearly simultaneous formation timing. Consequently, ADS 1693 emerges not as a quintuple but maybe as a physical triple system, with ADS 1693A (GZ And) as a W-subtype contact binary at its core and ADS 1693B acting as a distant companion orbiting the central binary.

Data availability statement

Publicly available datasets were analyzed in this study. These data can be found at: https://mast.stsci.edu/portal/Mashup/Clients/Mast/Portal.html.

Author contributions

L-QJ: Writing–original draft and writing–review and editing. JZ: Writing–review and editing.

Funding

The author(s) declare that financial support was received for the research, authorship, and/or publication of this article. This research was supported by the Joint Research Fund in Astronomy (Grant No. U1631108) under a cooperative agreement between the National Natural Science Foundation of China (NSFC) and the Chinese Academy of Sciences (CAS) and the Chinese National Natural Science Foundation of China (Grant No. 12103030). This work was partially supported by the Open Project Program of the Key Laboratory of Optical Astronomy, National Astronomical Observatories, Chinese Academy of Sciences.

Acknowledgments

We appreciate the valuable comments from anonymous referees, which have greatly improved the quality of our manuscript. This research has made use of the SIMBAD database, operated at CDS, Strasbourg, France. This paper has made use of data collected by the Transiting Exoplanet Survey Satellite (TESS) mission, for which funding is provided by the NASA Explorer Program. We acknowledge the support of the staff of the Xinglong 85-cm telescope.

Conflict of interest

The authors declare that the research was conducted in the absence of any commercial or financial relationships that could be construed as a potential conflict of interest.

Publisher's note

Supplementary material

The Supplementary Material for this article can be found online at: https://www.frontiersin.org/articles/10.3389/fspas.2024.1402031/full#supplementary-material

References

Baran, A., Zola, S., Rucinski, S. M., Kreiner, J. M., Siwak, M., and Drozdz, M. (2004). Physical parameters of components in close binary systems: II. *Acta Astron.* 54, 195–206.

Bertin, E., and Arnouts, S. (1996). SExtractor: software for source extraction. *Astronomy Astrophysics Suppl.* 117, 393–404. doi:10.1051/aas:1996164

Chambliss, C. R. (1992). Eclipsing binaries in multiple star systems. *Publ. Astronomical Soc. Pac.* 104, 663. doi:10.1086/133036

Collaboration, L., Cardoso, J. V. d. M., Hedges, C., Gully-Santiago, M., Saunders, N., Cody, A. M., et al. (2018). Lightkurve: Kepler and TESS time series analysis in Python. *Astrophys. Source Code Libr. Rec. ascl:1812.013.*

Cui, X.-Q., Zhao, Y.-H., Chu, Y.-Q., Li, G.-P., Li, Q., Zhang, L.-P., et al. (2012). The Large sky Area multi-object fiber spectroscopic telescope (LAMOST). *Res. Astronomy Astrophysics* 12, 1197–1242. doi:10.1088/1674-4527/12/9/003

Duchêne, G., and Kraus, A. (2013). Stellar multiplicity. *Annu. Rev. Astronomy Astrophysics* 51, 269–310. doi:10.1146/annurev-astro-081710-102602

Espin, T. E. (1908). Notes on double stars. *J. R. Astronomical Soc. Can.* 2, 248.

Gaia, C., Prusti, T., de Bruijne, J. H. J., Brown, A. G. A., Vallenari, A., Babusiaux, C., et al. (2016). The Gaia mission. *Astronomy Astrophysics* 595, A1. doi:10.1051/0004-6361/201629272

Gaia, C., Vallenari, A., Brown, A. G. A., Prusti, T., de Bruijne, J. H. J., Arenou, F., et al. (2023). Gaia Data Release 3. Summary of the content and survey properties. *Astronomy Astrophysics* 674, A1. doi:10.1051/0004-6361/202243940

Guinan, E. F. (2004). Seeing double in the local group: extragalactic binaries. *New Astron. Rev.* 48, 647–658. doi:10.1016/j.newar.2004.03.016

Jiang, L. Q., Qian, S. B., Zhang, J., and Zhou, X. (2015). 1SWASP J074658.62+224448.5: a low mass-ratio contact binary at the period cutoff. *Astronomical J.* 149, 169. doi:10.1088/0004-6256/149/5/169

Kouzuma, S. (2019). Starspots in contact and semi-detached binary systems. *Publ. Astronomical Soc. Jpn.* 71, 21. doi:10.1093/pasj/psy140

Kozai, Y. (1962). Secular perturbations of asteroids with high inclination and eccentricity. *Astronomical J.* 67, 591–598. doi:10.1086/108790

Kukarkin, B. V., Kholopov, P. N., Kukarkina, N. P., and Perova, N. B. (1975). 60th name-list of variable stars. *Inf. Bull. Var. Stars* 961, 1.

Liu, X., Yang, J., and Tan, H. (1987). New UBV photoelectric observations of GZ and. *Inf. Bull. Var. Stars* 3080, 1.

Lu, W., and Rucinski, S. M. (1999). Radial velocity studies of close binary stars. I. *Astronomical J.* 118, 515–526. doi:10.1086/300933

Lucy, L. B. (1967). Gravity-darkening for stars with convective envelopes. *Z. für Astrophys.* 65, 89.

Mowlavi, N., Holl, B., Lecoeur-Taïbi, I., Barblan, F., Kochoska, A., Prša, A., et al. (2023). Gaia Data Release 3. The first Gaia catalogue of eclipsing-binary candidates. *Astronomy Astrophysics* 674, A16. doi:10.1051/0004-6361/202245330

O'Connell, D. J. K. (1951). The so-called periastron effect in close eclipsing binaries; New variable stars (fifth list). *Publ. Riverv. Coll. Observatory* 2, 85–100.

Prša, A., Kochoska, A., Conroy, K. E., Eisner, N., Hey, D. R., Ijspeert, L., et al. (2022). TESS eclipsing binary stars. I. Short-Cadence observations of 4584 eclipsing binaries in sectors 1-26. *Astrophysical J. Suppl. Ser.* 258, 16. doi:10.3847/1538-4365/ac324a

Qian, S.-B., He, J.-J., Zhang, J., Zhu, L.-Y., Shi, X.-D., Zhao, E.-G., et al. (2017). Physical properties and catalog of EW-type eclipsing binaries observed by LAMOST. *Res. Astronomy Astrophysics* 17, 087. doi:10.1088/1674-4527/17/8/87

Qian, S. B., Zhang, J., He, J. J., Zhu, L. Y., Zhao, E. G., Shi, X. D., et al. (2018). Physical properties and evolutionary States of EA-type eclipsing binaries observed by LAMOST. *Astrophysical J. Suppl. Ser.* 235 (5), 5. doi:10.3847/1538-4365/aaa601

Ricker, G. R., Winn, J. N., Vanderspek, R., Latham, D. W., Bakos, G. Á., Bean, J. L., et al. (2015). Transiting Exoplanet survey satellite. *J. Astronomical Telesc. Instrum. Syst.* 1, 014003. doi:10.1117/1.JATIS.1.1.014003

Ruciński, S. M. (1969). The proximity effects in close binary systems. II. The bolometric reflection effect for stars with deep convective envelopes. *Acta Astron.* 19, 245.

Slawson, R. W., Prša, A., Welsh, W. F., Orosz, J. A., Rucker, M., Batalha, N., et al. (2011). Kepler eclipsing binary stars. II. 2165 eclipsing binaries in the second data Release. *Astronomical J.* 142, 160. doi:10.1088/0004-6256/142/5/160

Tokovinin, A., Thomas, S., Sterzik, M., and Udry, S. (2006). Tertiary companions to close spectroscopic binaries. *Astronomy Astrophysics* 450, 681–693. doi:10.1051/0004-6361:200544270004-6361:20054427

Torres, G., Andersen, J., and Giménez, A. (2010). Accurate masses and radii of normal stars: modern results and applications. *Astronomy Astrophysics Rev.* 18, 67–126. doi:10.1007/s00159-009-0025-1

van Hamme, W. (1993). New limb-darkening coefficients for modeling binary star light curves. *Astronomical J.* 106, 2096. doi:10.1086/116788

Walker, R. L. (1973). A newly discovered W ursae majoris system: ADS 1693 A. *Inf. Bull. Var. Stars* 855 (1).

Walker, R. L. (1991). GZ and = ADS 1693, A quintuplet system. *Bull. Am. Astronomical Soc.* 23, 881.

Walker, R. L. (1996). GZ Andromeda, the more the merrier. *Bull. Am. Astronomical Soc.* 28, 921.

Wang, Z.-H., and Zhu, L.-Y. (2021). Is the eclipsing binary RR Dra dancing with a hidden tertiary black hole candidate? *Mon. Notices R. Astronomical Soc.* 507, 2804–2812. doi:10.1093/mnras/stab2356

Wang, Z. H., Zhu, L. Y., and Yuan, K. (2022). Characterizing non-thermal equilibrium contact binaries. *Mon. Notices R. Astronomical Soc.* 517, 1007–1019. doi:10.1093/mnras/stac2629

Welsh, W. F., Orosz, J. A., Carter, J. A., Fabrycky, D. C., Ford, E. B., Lissauer, J. J., et al. (2012). Transiting circumbinary planets Kepler-34 b and Kepler-35 b. *Nature* 481, 475–479. doi:10.1038/nature10768

Wilson, R. E., and Devinney, E. J. (1971). Realization of accurate close-binary light curves: application to MR cygni. *Astrophysical J.* 166, 605. doi:10.1086/150986

Wilson, R. E., and Van Hamme, W. (2014). Unification of binary star ephemeris solutions. *Astrophysical J.* 780, 151. doi:10.1088/0004-637X/780/2/151

Yang, Y., and Liu, Q. (2003). An abnormal radiant luminosity of the contact binary GZ Andromedae and its possible explanation. *Astronomy Astrophysics* 401, 631–637. doi:10.1051/0004-6361:20030061

Zhao, G., Zhao, Y.-H., Chu, Y.-Q., Jing, Y.-P., and Deng, L.-C. (2012). LAMOST spectral survey — an overview. *Res. Astronomy Astrophysics* 12, 723–734. doi:10.1088/1674-4527/12/7/002

Zhou, A.-Y., Jiang, X.-J., Zhang, Y.-P., and Wei, J.-Y. (2009). MiCPhot: a prime-focus multicolor CCD photometer on the 85-cm Telescope. *Res. Astronomy Astrophysics* 9, 349–366. doi:10.1088/1674-4527/9/3/010

Zhou, X., Qian, S., He, J., Zhang, J., and Jiag, L. (2015). The first four-color photometric investigation of the W UMa type contact binary V868 Monocerotis. *Publ. Astronomical Soc. Jpn.* 67, 98. doi:10.1093/pasj/psv067

Zhou, X., Qian, S. B., Zhang, J., Jiang, L. Q., Zhang, B., and Kreiner, J. (2016). A solar-type stellar companion to a deep contact binary in a quadruple system. *Astrophysical J.* 817, 133. doi:10.3847/0004-637X/817/2/133

Zhou, X., and Soonthornthum, B. (2019). The W-subtype active contact binary PZ UMa with a possible more massive tertiary component. *Publ. Astronomical Soc. Jpn.* 71, 39. doi:10.1093/pasj/psz003

Zhou, X., Soonthornthum, B., Qian, S. B., and Fernández Lajús, E. (2019). V752 Cen - a triple-lined spectroscopic contact binary with sudden and continuous period changes. *Mon. Notices R. Astronomical Soc.* 489, 4760–4770. doi:10.1093/mnras/stz2508